Proceeding of the IEEE
International Conference on Robotics and Biomimetics
Dali, China, December 2019

An Active Compliance Controller-based Autonomous Assistive Robotic System for Beard Shaving of People with Disabilities

Ajani S. Oladayo[1] and Samy F. M. Assal[2]

***Abstract*— The potential of using robotic systems to provide assistance for people with disabilities that result from neurological disorders or several other diseases is increasing fast. Specifically, people with arm disabilities are receiving robotic assistance in several daily living activities such as shaving, eating, brushing and drinking. Due to the increased complexities and risks associated with the use of fully autonomous robotic system to tackle this problem, the shared controlled or active robotic systems are used mainly to provide such assistance. In this work, an autonomous robotic system for beard shaving assistance is presented taking into account the complexity and bringing the risks to the barest minimum by introducing an active compliance control scheme. A Kinect RGB-D sensor is utilized to detect the patients face, recognize and segment the bearded regions based on selected geometrical features and subsequently plan optimal trajectories for fulfilling the intended shaving task. The system is capable of online replanning optimal trajectories in case of unintentional head pose changing, loss of contact and occlusion. Based on the full dynamic of the UR-10 six DOF manipulator using ADAMS and MATLAB, an impedance controller whose parameters are obtained using Genetic Algorithm (GA) with force/torque constraints is developed. The Simulation results demonstrate the capability of the proposed system to achieve beard shaving autonomously that could be extended for fulfilling other tasks around the head.**

I. INTRODUCTION

Assistive robotics is the area of robotics where robotic systems are developed to provide assistance for people with severe manipulation and mobility challenges in order to improve their quality of life and independence [1]. Several levels of assistance and rehabilitation have been studied using serial and parallel manipulators [2], [3], [4]. Recently, for people with disabilities of arm, shoulder and hand, the potential of using robotic systems to provide assistance in several daily live activities (ADL) such as eating, drinking, beard shaving and brushing has been increased extremely. This can be asserted by a number of recent works such as robot-assisted feeding, drinking, shaving, scratching and brushing [5], [6], [7], [8]. A scooping review of existing robotic systems for assistance in terms of ADLs was presented in [9]; in which some of these systems have been classified and evaluated in terms of their ease of use and safety, interfacing and control, economic feasibility and task prioritization.

The limitation of these existing systems is that they are developed on the assumptions that patients are able to participate in the control of these systems. Thus, these systems are either manually controlled by the patients via input interfaces, interactive such that patients have to be interactive with them to perform ADLs or controlled through a shared control scheme. Although having fully autonomous systems to provide such assistance will eliminate the defects of the existing systems, such systems are limited in design due to increased complexities, safety and efficiency issues [6]. For example, an intricate coordination of contact force and motion generation for performing selected tasks, which requires sophisticated control algorithms, have to be developed [10].

Amidst several other ADLs which are performed around the head, shaving and scratching have been rated as high priority tasks [11]. A shared control robotic system was developed in [5] to perform shaving and scratching; in which the user was allowed to select the desired tool position from a graphical interface to plan the desired trajectories. Also, based on the assumption that a patient has full control of his/her head motion, an ellipsoidal model for user head registration was adopted to position the shaving tool near the users head and thus enabling the user to move his chin to rub the tool [6]. Poor shaving of over 40 minutes shaving time was recorded in [5] and [6] due to irregular force application.

The allowable force range for tasks involving human-robot interaction is from 2N to 10N as recommended [12]. This force range was investigated in [13] and applied by [5] for robot assisted shaving, where a withdrawal mechanism was designed such that when the allowable force is reached or exceeded, the robot withdraws from the human. This isn't safe enough and does not guarantee good shaving because no desired force trajectory is specified.

Although it has been indicated that, the full potential of the use of general purpose robot to provide assistance lies in its high autonomy, the complexities involved in the realization of such autonomy level are not trivial. Considering that intricate coordination of contact force and motion generation is required, compliance control becomes a necessity here. Generally compliance can be introduced to a system through active or passive compliance [10]. Passive compliance is basically introduced into a system as compliant mechanical elements; while active compliance can be introduced through active interaction control schemes. The most efficient active compliance is the impedance control which mimics human

[1]Ajani S. Oladayo is with the Department of Mechatronics and Robotics Engineering, School of Innovative Design Engineering, Egypt - Japan University of Science and Technology (E-JUST), Alexandria, Egypt. oladayo.solomon@ejust.edu.eg

[2]Samy F. M. Assal is with the Department of Mechatronics and Robotics Engineering, School of Innovative Design Engineering, Egypt - Japan University of Science and Technology (E-JUST), Alexandria, Egypt.; on leave from the Department of Production Engineering and Mechanical Design, Faculty of Engineering, Tanta University, Egypt samy.assal@ejust.edu.eg

978-1-7281-6321-5/19//$31.00 ©2019 IEEE

behavior by imposing mass-spring-damper-like disturbance response. So in this paper, rather than the active assistive robotic systems with no compliance, the work in [14] is extended to an active compliance robotic system that is capable of performing autonomous and reliable beard shaving assistance by extending the existing technology for autonomous face detection and tracking, beard region recognition, trajectory planning and impedance control based on the robot dynamics is presented. In the proposed system, A Kinect RGB-D sensor and a general purpose UR-10 robot with an attached circular trimming tool are proposed as a platform for achieving the beard shaving task. Also, the selection of the position of the robotic system fixed base enabling both sides of the face to be shaved as well as camera occlusion are taken into consideration. Additionally, attention has been taken for the online re-planning of the optimal trajectories once the pose of the patient face changes. Furthermore, the performance of the proposed active impedance is evaluated in terms of tracking the generated shaving trajectories and the desired force trajectory by co-simulating the full dynamics of the proposed system in ADAMS and MATLAB.

The rest of this paper is organized as follows, an overview of the the proposed robotic system is discussed in Section II. Section III gives details on face detection and beard region estimation. In Section IV, the analysis of obtaining the required orientation of the robot end-effector and trajectory planning are detailed. The dynamic model of the robotic system in ADAMS and the impedance control are discussed in Section V. Consequently, results of tracking trajectories with the required force are discussed in Section VI. Finally, conclusions and future work are presented in Section VII.

II. Overview of the Robotic System

The proposed robotic system consists of the 6-DOF UR10 collaborative robot, with an electric shaving tool fixed at the end-effector and a vision sub system which is a kincet RGB-D sensor as shown in Fig 1. The choice of the position of the fixed robotic base is based on performing the whole shaving operation of both sides of the face from one base location and bringing the occlusion to the barest minimum. Therefore the position of the camera and UR10 robot base are chosen to be at the sagittal plane of the patient and the camera should be tilted to cover the robot workspace.

To achieve autonomous beard shaving, the 3D point positions within the bearded area of the patients face and the desired end-effector orientation required to position the trimmer normal to the face surface at those points are needed to be known to enable planning different trajectories for the shaving task. Thus the Kinect RGB-D sensor is used for face detection and tracking. Also, the 1347 3D facial point-cloud distribution from the kinect sensor is employed to achieve beard detection and region estimation. The point positions obtained from these steps are defined with respect to the camera coordinate frame. Hence, transformations between the camera frame and the robot base frame are also carried out. To determine the desired end-effector orientation required to align the shaving tool normal to the face surface at those

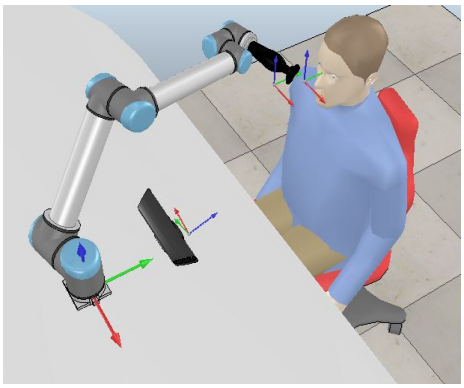

Fig. 1: Overview of the proposed robotic system setup with coordinate frames.

points, the surface normal of each of the facial points within the beard region are obtained. Consequently, transformations are carried out to obtain the desired orientation of the end-effector with respect to the base of the robot. The resulting point positions and end-effector orientations are set as inputs to the trajectory planner which plans the required trajectories to complete the shaving task. These trajectories are fed as input to the robot controller which is a force tracking-based impedance controller that is based on the dynamics of the UR10 robot co-simulated in ADAMS and MATLAB.

III. Face Detection and Beard Region Estimation

This section focuses on computing the desired end-effector positions and orientations required to complete the shaving task, which infact are the positions of the points within the beard region of the face and the orientations based on the normal to the face surface at these facial points.

A. Face Detection and tracking

The kinect RGB-D sensor captures both depth and colour images using its infrared (IR) and RGB camera respectively. The Application Programming Interface (API) of Microsoft, which is called HD face and contains a face detection and tracking engine [15], is used to capture the face and create a point-cloud that represents it as shown in Fig. 2.

Fig. 2: Illustration of the face detection for two different instances showing a point-cloud model distribution of 1347 points which represent the face

This is efficient for the proposed system because the camera returns the 3D point-cloud information of the detected face in a matrix form as $P \in \Re^{3X1347}$, where the matrix

row represents the XYZ coordinate of the facial point and the matrix column is the index label of each point. Kin2, a Kinect 2 toolbox for MATLAB is used to implement this process [16]

B. Beard Region Estimation

1) Beard Detection: To determine the bearded region, the face is examined first if it is beard or not. The beard detection is carried based on the analysis of the some geometric properties of the facial points surface normal. Obtaining the normal vectors is equivalent to the least-square plane fitting estimation problem which can be solved using the function "pcnormals" in MATLAB. The function uses six neighboring points to fit a local plane to determine each normal vector for a set of input point-cloud data. Essentially, there is no mathematical way to compute for the direction of normal, thus the directions of the normals obtained are not consistently oriented over the entire point-cloud data. This problem becomes trivial if the viewpoint of the sensor $\boldsymbol{v}_p$ is in fact known. To orient all normals $\boldsymbol{n}_i$ consistently towards the viewpoint, they need to satisfy the following

$$\boldsymbol{n}_i \cdot (\boldsymbol{v}_p - \boldsymbol{p}_i) > 0 \tag{1}$$

The process involved in the correction of the directions of the normal vectors based on (1) is illustrated by Algorithm 1. Figure 3 shows the normals to the points on the face surface before and after direction correction.

Algorithm 1: Pseudo-code showing the correction of the direction of the normal vectors

Input : $\boldsymbol{n}_i$, $\boldsymbol{v}_p$, $\boldsymbol{p}_i$
Output: $\boldsymbol{n}_i \in \Re^3$ $for\ i = 1, ..., 1347$
$D_i \leftarrow \boldsymbol{n}_i.(\boldsymbol{v}_p - \boldsymbol{p}_i)$;
if $D_i > 0$ **then**
  return $\boldsymbol{n}_i = \boldsymbol{n}_i$
else
  return $\boldsymbol{n}_i = -\boldsymbol{n}_i$
end

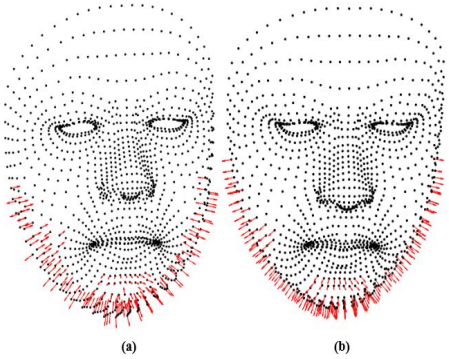

Fig. 3: Representative face surface normals, before and after direction correction: (a) before, (b) after

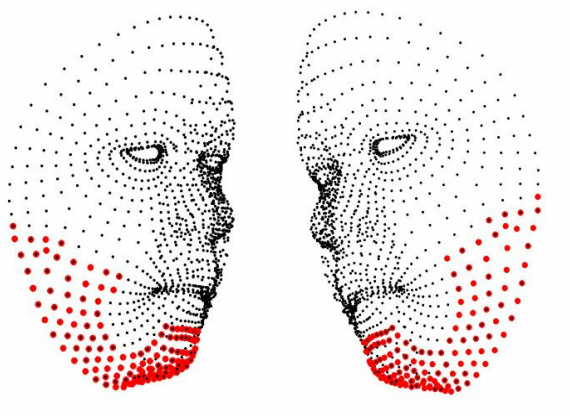

Fig. 4: Illustration of extracted beard region shown in red for left and right sides of the face

Based on the standard deviation of the angles of the normal vectors for each K nearest neighborhood, the face can be classified as beard or not. This can be achieved by computing the angles between face surface normal vectors (ANV) with common edges. Then, the sum of angles of each set of the k six nearest neighborhood normal vectors (SANV) is calculated and known thresholds of this standard deviation can be used to determined if the face is a bearded face or not [17].

2) Beard region Estimation: Colour-based segmentation has been widely studied for beard segmentation since the beard is always gray in terms of colour, and thus carefully selected thresholds can be used to segment the region of interest (ROI). Edge detection-based segmentation has also been used but both of these approaches often fails in the presence of shadows and illumination artifacts [18]. To over come the drawback of discontinuity, spare classifier was used in [19] but this approach is time consuming and hence not suitable for real-time applications. Therefore rather than colour- or edge-based segmentation which is often used in unconstrained background for 2D segmentation, 3D semantic segmentation based on the known labels of each point on the face is proposed to be used here.

The label of each points in the point-cloud of the face can be used to segment the face and extract the beard region. The beard region segmentation is based on the observation that the bearded region of the face or the shaving area falls within known segments of the face. Thus the labels of these regions are considered as labels for the bearded region as illustrated in Fig. 4. Then, all the facial points within this bounded region are used as the 3D position points of the beard.

IV. End-Effector Orientation and Trajectory Planing

A. End-Effector Orientation

Since the normal to the surface of face is known for each point $\boldsymbol{p}_i$ within the bearded area with respect to the camera frame C, and the tool attached to the end-effector should be

aligned to this normal. The required end-effector orientation to achieve this can be calculated with respect to the base coordinate frame of the robot B by solving for the rotation matrix ${}^{C}\mathrm{R}_{E}$, from which the Roll-Pitch and Yaw angles can be obtained. Consequently transformations from the camera frame to the robot base frame can be applied. From Fig. 5, the rotational matrix ${}^{C}\mathrm{R}_{E}$, can be obtained as follows

$$\boldsymbol{r}_a = \boldsymbol{r}_{pi} + {}^{C}\mathrm{R}_{E}\ {}^{E}\boldsymbol{n}_i \tag{2}$$

where a is an arbitrary point on the normal $\boldsymbol{n}_i$, $\boldsymbol{r}_a$ is the position vector of point a with respect to frame C, $\boldsymbol{r}_{pi}$ is the position vector of $\boldsymbol{p}_i$ with respect to frame C. Since the tool is fixed to the frame E, ${}^{E}n_i$ is constant and it is assumed to be known. Thus, the rotation matrix ${}^{C}\mathrm{R}_{E}$ can be obtained from (2), the Roll-pitch-Yaw angles of this rotational matrix ${}^{K}\mathrm{R}_{E}$ can be determined by solving a set of three nonlinear algebraic equations defined by (2). The

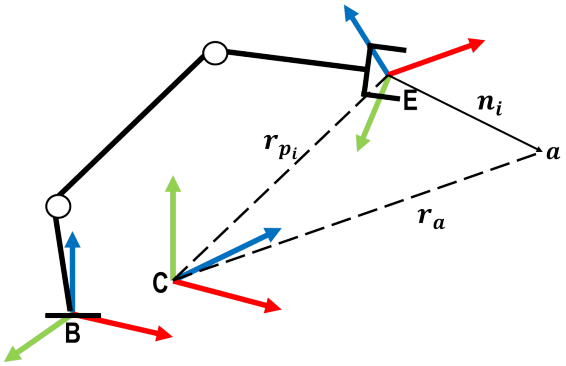

Fig. 5: End-effector orientation

desired rotational matrix of the end-effector E with respect to the manipulator based frame B (${}^{B}\mathrm{R}_{E}$) can be obtained by applying the transformation given in (3). Thus, the desired pose of the end-effector at each point $\boldsymbol{p}_i$ on the shaving area can be obtain. This paves way for planning trajectories within the bounded shaving area for the trimming tool to track.

$${}^{B}\mathrm{R}_{E} = {}^{B}\mathrm{R}_{K}\ {}^{k}\mathrm{R}_{E} \tag{3}$$

B. Trajectory Planing

Since the desired pose of the end-effector $\boldsymbol{x}_i$ at each point $\boldsymbol{p}_i$ within the shaving areas is obtained, optimal trajectories can be planned to achieve the shaving task. Cubic spline which can satisfy smooth and continuous trajectories $\boldsymbol{x}(t)$ with zero initial and final velocities are used and the via points are carefully selected based on beard maps. Beard map shows how facial hair grows and in which direction the tool should move over the bearded area to obtain optimal shaving.

The desired force F_d is considered only in the Z-direction of the robot end-effector as this is the required force-controlled direction to complete a clean shaving.

V. Robot Dynamics and Force Tracking-Based Impedance Control

A. Robot Dynamic Model

The dynamic equations of an n DOF robot manipulator can be written generally as

$$M(\boldsymbol{q})\ddot{\boldsymbol{q}} + C(\boldsymbol{q},\dot{\boldsymbol{q}})\dot{\boldsymbol{q}} + g(\boldsymbol{q}) = \boldsymbol{\tau}_m - \boldsymbol{\tau}_{ext} \tag{4}$$

where $\boldsymbol{q},\dot{\boldsymbol{q}},\ddot{\boldsymbol{q}} \in \mathbb{R}^n$ are the joint position, velocity and acceleration vectors respectively; $M(\boldsymbol{q}) \in \mathbb{R}^{n\times n}$ is the mass matrix; $C(\boldsymbol{q},\dot{\boldsymbol{q}})\dot{\boldsymbol{q}} \in \mathbb{R}^n$ denotes the Coriolis and centrifugal vector; $g(\boldsymbol{q}) \in \mathbb{R}^n$ is the gravity vector; $\boldsymbol{\tau}_m \in \mathbb{R}^n$ is the motor torque vector which is the control input and $\boldsymbol{\tau}_{ext} = J^T(\boldsymbol{q})\boldsymbol{f}_{ext} \in \mathbb{R}^n$, in which $\boldsymbol{f}_{ext} \in \mathbb{R}^m$ denotes the external force measured in the m-Cartesian space and mapped to the joint space with the Jacobian transpose $J^T(\boldsymbol{q}) \in \mathbb{R}^{n\times m}$

For high number of n DOF and irregular shape manipulators, obtaining (4) using either the Lagrange or the Newton-Euler method becomes often difficult. So, ADAMS software is used here to dynamic simulate the UR10 6-DOF manipulator. First, the robot CAD model obtained from the manufacturer in Solidworks is exported to ADAMS. In ADAMS, revolute joints are added to each of the joint locations with necessary inputs and measurements parameters set, thereafter the model is exported to MATLAB for co-simulation between ADAMS and MATLAB, which is important for achieving virtual environment for validating different control schemes. As illustrated in Fig 6 input torques in ADAMS are supplied from MATLAB as variables based on the control architecture while the outputs of this model are basically the joint angles, velocities and accelerations.

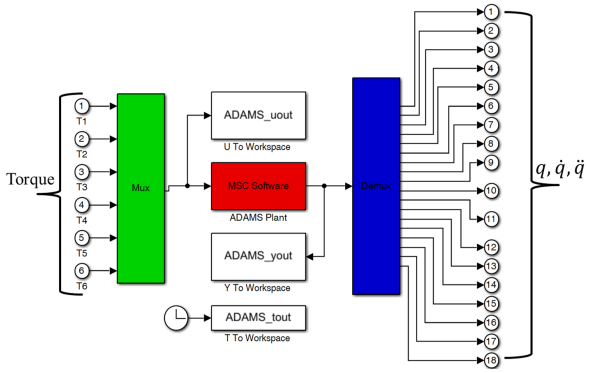

Fig. 6: Exported Adams Dynamic Block

B. Force Tracking-based Impedance Control

In the shaving task, the interaction required between the manipulator and the human is basically a force-position relation. Impedance control provides effectively this level of interaction because it enables motion trajectory tracking and realizes a desired dynamic interaction between the end-effector position and the contact force [20], [21]. The desired dynamic behavior between the interaction force of the trimmer and desired trajectory within the bearded region can be modeled as follows

$$f_d - f = K_d(\boldsymbol{x}_d - \boldsymbol{x}) + B_d(\dot{\boldsymbol{x}}_d - \dot{\boldsymbol{x}}) + M_d(\ddot{\boldsymbol{x}}_d - \ddot{\boldsymbol{x}}) \quad (5)$$

where K_d, B_d, M_d are the desired stiffness, damping and inertia impedance diagonal matrices respectively; generally, $M_d = 0$ is assumed. f_d is the desired interaction force between the trimmer and the human. The block diagram of the closed loop impedance control system is shown in Fig. 7.

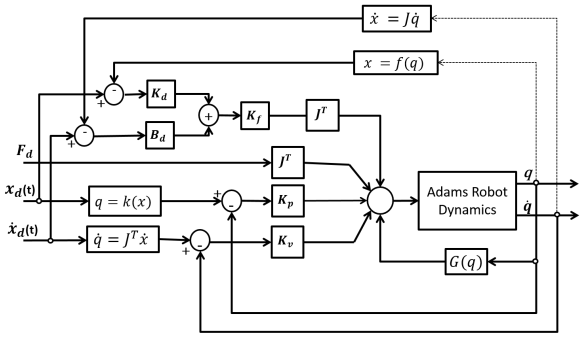

Fig. 7: Closed loop active impedance control

The impedance control law is given as follows

$$U = J^T(\boldsymbol{q})[K_p(\boldsymbol{x}_d - \boldsymbol{x}) + K_v(\dot{\boldsymbol{x}}_d - \dot{\boldsymbol{x}}) + f_d + K_f(f_d - f)] + G \quad (6)$$

where K_f, K_p and K_v are force, position and velocity gain diagonal matrices respectively. Since

$$(\boldsymbol{x}_d - \boldsymbol{x}) \approx J(\boldsymbol{q}_d - \boldsymbol{q}) \quad (7)$$

and

$$J^T(\boldsymbol{q})K_p(\boldsymbol{x}_d - \boldsymbol{x}) = K_p(\boldsymbol{q}_d - \boldsymbol{q}) \quad (8)$$

Therefore, (6) can be rewritten as

$$U = K_p(\boldsymbol{q}_d - \boldsymbol{q}) + K_v(\dot{\boldsymbol{q}}_d - \dot{\boldsymbol{q}}) + J^T(\boldsymbol{q})[f_d + K_f(f_d - f)] + G \quad (9)$$

For the controller to be asymptotically stable, the following conditions must be satisfied as proposed in [22].

$K_p + (I + K_f)K_d > 0$, $K_v + (I + K_f)B_d > 0$, $M_d = 0$

or

$K_p > 0$, $K_v > 0$, $K_f = -1$

1) GA-based Gains Tuning: since classical tuning approaches such as Nichols and Ziegler cannot be used to obtain the optimal controller gains, meta-heuristic optimization techniques such as GA, SA or PSO can be used. GA which is based on natural selection and genetics is proposed to be used in this study because GA is faster than SA and does not tend to have problem of premature convergence as PSO. The objective function which minimizes the tracking error $\boldsymbol{e} = \boldsymbol{x}_d - \boldsymbol{x}$ and settling time t_s is given as [23]

$$F_{obj} = t_s + \int_0^\infty \boldsymbol{e}^T(t)\boldsymbol{e}(t) \quad (10)$$

The range of the controller gains K_p can be specified as a lower and upper limits in the GA parameters. In order to determine this range, a basic control algorithm is used in ADAMS yielding the lower limit as diag[1000 40000 15000 500 20 10] and upper ones as diag[2500 60000 25000 1000 80 50]

VI. Results and Discussion

Impedance control based on the full dynamics of the UR10 manipulator is used in Co-simulations between ADAMS and MATLAB Simulink® installed on an intel core(TM) i7-4790, 3.60GHz processor. The desired stiffness and damping matrices, K_d and B_d are chosen as diag[0 0 400 0 0 0] and diag[0 0 20 0 0 0] respectively. The desired force f_d is also chosen as diag[0 0 2 0 0 0]. The gains obtained from GA; namely, K_p and K_v used in this simulation are diag[2000 50000 20000 800 50 25] and diag[0.4 5 1.5 0.025 0.005 0.0018] respectively.

The position and force trajectories are set as inputs to the impedance controller. Figure 8(a) - (c) shows the position tracking results of a sample trajectory in XYZ coordinates and Fig. 8(d)-(f) shows orientation tracking in terms of Roll, Pitch and Yaw angles respectively. Figure 9 shows that the force tracking error of $f_d - f$ in the Z direction which is regulated to zero over time and this ensures that shaving is performed with the desired force f_d.

VII. Conclusions

In this paper, an autonomous robotic system for face detection, beard region estimation and optimal trajectory planning for beard shaving assistance has been developed. On the context of developing this robotic system, an active impedance controller has been designed to achieve required impedance interaction between the manipulator and the human. Also, the execution at the desired force ensures system safety and effectiveness in terms of clean shaving. In future, intelligence shall be introduced to the impedance control for unknown environments.

Acknowledgment

This research is supported by Egypt Ministry of Higher Education through Egypt-Japan University of Science and Technology Scholarship for the first author.

References

[1] D. J. Weber, B. A. Salatin, and G. G. Grindle, "The Role of Assistive Robotics in the Lives of Persons with Disability." *American Journal of Physical Medicine & Rehabilitation*, pp. 509–521, 2010.

[2] A. Asker, S. F. Assal, and A. M. Mohamed, "Dynamic Analysis of a Parallel Manipulator-Based Multi-function Mobility Assistive Device for Elderly," *Proceedings - 2015 IEEE International Conference on Systems, Man, and Cybernetics, SMC 2015*, pp. 1409–1414, 2015.

[3] A. Asker, S. F. M. Assal, M. Ding, J. Takamatsu, and A. M. Mohamed, "Modeling of natural sit-to-stand movement based on minimum jerk criterion for natural-like assistance and rehabilitation," *Advanced Robotics*, vol. 31, no. 17, pp. 901–917, October, 2017.

[4] A. Asker and S. F. Assal, "Kinematic Analysis of a Parallel Manipulator-Based Multi-Function Mobility Assistive Device for Elderly," *2015 IEEE/ASME International Conference on Advanced Intelligent Mechatronics (AIM)*, pp. 676–681, 2015.

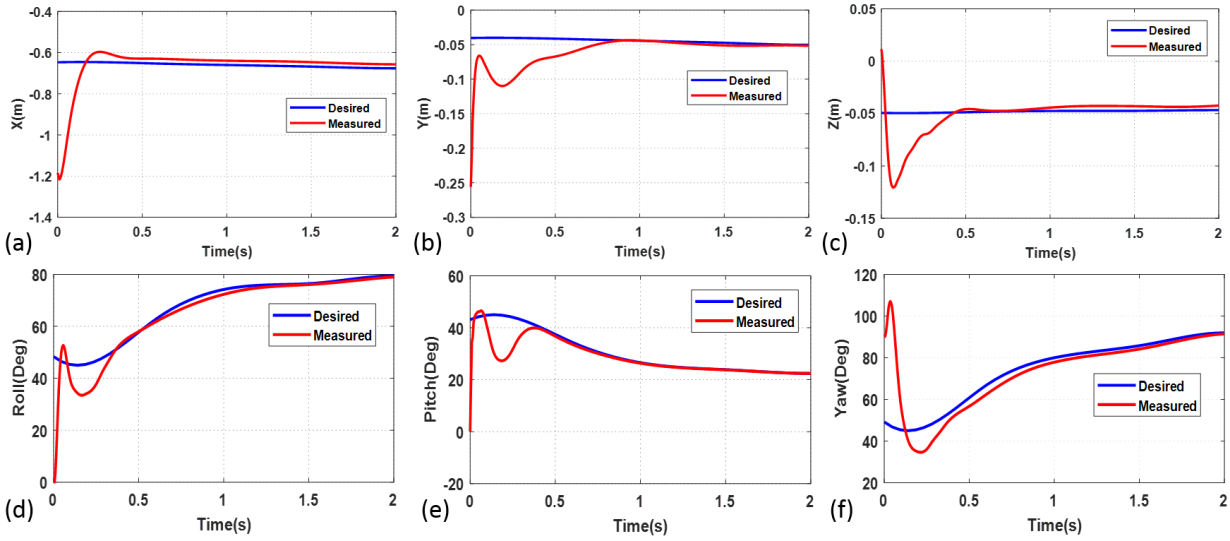

Fig. 8: Co-simulation Results from Position and Orientation: (a) Position tracking in X (b) Position tracking in Y (c) Position tracking in Z (d) Roll orientation tracking (e) Pitch orientation tracking (f) Yaw orientation tracking

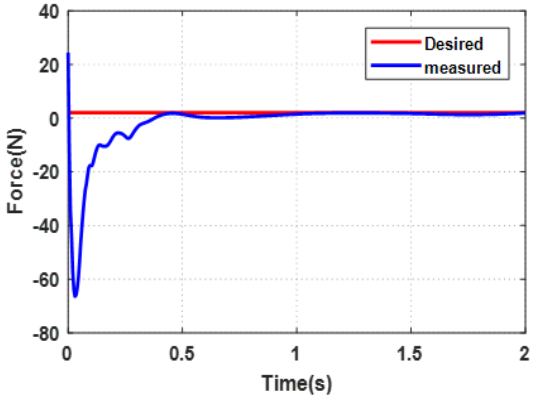

Fig. 9: Force Tracking Results

[5] T. L. Chen, M. Ciocarlie, S. Cousins, P. Grice, K. Hawkins, K. Hsiao, C. Kemp, C. H. King, D. Lazewatsky, A. E. Leeper, H. Nguyen, A. Paepcke, C. Pantofaru, W. Smart, and L. Takayama, "Robots for humanity: Using assistive robotics to empower people with disabilities," *IEEE Robotics and Automation Magazine*, vol. 20, no. 1, pp. 30–39, 2013.

[6] K. P. Hawkins, P. M. Grice, T. L. Chen, C. H. King, and C. C. Kemp, "Assistive mobile manipulation for self-care tasks around the head," *IEEE Symposium on Computational Intelligence in Robotic Rehabilitation and Assistive Technologies*, pp. 16–25, 2014.

[7] S. Schröer, I. Killmann, B. Frank, M. Völker, L. Fiederer, T. Ball, and W. Burgard, "An autonomous robotic assistant for drinking," *Proceedings - IEEE International Conference on Robotics and Automation*, pp. 6482–6487, 2015.

[8] A. Candeias, T. Rhodes, and M. Marques, "Vision augmented robot feeding," *European Conference on Computer Vision*, pp. 50–65, 2016.

[9] A. Bilyea, N. Seth, S. Nesathurai, and H. A. Abdullah, "Robotic assistants in personal care: A scoping review," *Medical Engineering and Physics*, vol. 49, pp. 1–6, 2017.

[10] C. Schindlbeck and S. Haddadin, "Unified Passivity-Based Cartesian Force / Impedance Control for Rigid and Flexible Joint Robots via Task-Energy Tanks," *IEEE International Conference on Robotics and Automation (ICRA)*, pp. 440–447, 2015.

[11] T. L. Chen, M. Ciocarlie, S. Cousins, P. Grice, K. Hawkins, K. Hsiao, C. C. Kemp, C.-h. King, D. A. Lazewatsky, A. Leeper, H. Nguyen, A. Paepcke, C. Pantofaru, W. D. Smart, and L. Takayama, "Robots for Humanity : A Case Study in Assistive Mobile Manipulation," *IEEE Robotics & Automation Magazine, Special issue on Assistive Robotics*, 2013.

[12] Y. Tsumaki, T. Kon, A. Suginuma, K. Imada, A. Sekiguchi, D. N. Nenchev, H. Nakano, and K. Hanada, "Development of a skincare robot," *Proceedings - IEEE International Conference on Robotics and Automation*, pp. 2963–2968, 2008.

[13] M. Melia, M. Schmidt, B. Geissler, J. König, U. Krahn, H. J. Ottersbach, S. Letzel, and A. Muttray, "Measuring mechanical pain: The refinement and standardization of pressure pain threshold measurements," *Behavior Research Methods*, vol. 47, no. 1, pp. 216–227, 2015.

[14] A. S. Oladayo, S. F. M. Assal, and H. El-hussieny, "Towards Development of an Autonomous Robotic System for Beard Shaving Assistance for Disabled People," *IEEE International Conference on Systems, Man, and Cybernetics (SMC), Italy*, 2019.

[15] E. Tsakiraki, "Real-time Head Motion Tracking for Brain Positron Emission Tomography using Microsoft," Ph.D. dissertation, 2016.

[16] J. R. Terven and M. C. Diana, "Kin2 . A Kinect 2 Toolbox for MATLAB," *Science of Computer Programming*, 2017.

[17] R. Dhahri and S. Belaid, "A new method to detect and remove a beard from 3D human face model," *International Journal of Operational Research*, vol. 27, no. 1/2, p. 201, 2016.

[18] T. H. N. Le, K. Luu, C. Zhu, and M. Savvides, "Semi Self-Training Beard/Moustache Detection and Segmentation Simultaneously," *Image and Vision Computing*, no. 58, pp. 214–223, 2016.

[19] J. G. Wang and W. Y. Yau, "Real-time moustache detection by combining image decolorization and texture detection with applications to facial gender recognition," *Machine Vision and Applications*, vol. 25, no. 4, pp. 1089–1099, 2014.

[20] N. Hogan, "Impedance control of industrial robots," *Robotics and computer -integrated manufacturing*, vol. 1, no. 1, pp. 97–113, 1984.

[21] S. Jung, S. Y. Bin, and T. C. Hsia, "Experimental studies of neural network impedance force control for robot manipulators," in *IEEE International conference on robotics and automation*, 2001, pp. 3453–3458.

[22] H. Mehdi and O. Boubaker, "Stiffness and Impedance Control Using Lyapunov Theory for Robot-Aided Rehabilitation," *international Journal of Social Robotics*, no. 4, pp. 107–119, 2012.

[23] M. A. Naeem and S. F. M. Assal, "Development of a 4-DOF cane robot to enhance walking activity of elderly," *Proceedings of the Institute of Mechanical Engineers, Part C: Journal of Mechanical Engineering Sciences*, no. 0, pp. 1–19, 2019. [Online]. Available: 10.1177/0954406219830440